Emergent fluctuations at the hub of interaction

Yizhou Liu[1, 2, *]

[1] *Physics of Living Systems, Department of Physics, MIT, Cambridge, MA 02139, USA.*
[2] *Department of Mechanical Engineering, MIT, Cambridge, MA 02139, USA.*

(Dated: May 17, 2024)

Understanding the dynamics of hubs—central entities that interact with numerous other entities—is crucial across various fields, including ecology, transportation, and economy. Hubs can influence and be influenced by connected entities, and this interaction can lead to complex behaviors. To model these interactions, we propose a stochastic delay differential equation (SDDE) framework focusing on the hub's dynamics. This model incorporates delayed responses to reflect the time it takes for the hub to affect connected entities and for these entities to affect the hub back. Additionally, stochastic noise is included to account for various factors, such as weak inter-entity interactions. We specifically investigate the dynamics of hubs using numerical simulations and theoretical analysis, uncovering a range of emergent behaviors, including stable states, limit cycles, and chaos. The transition from stable states to limit cycles is explained by analyzing the linear dynamics—stronger total delay response strength, longer mean delay time, or higher delay time variance tend to lead to limit cycles. Transition to chaos is partly explained by the linear part analysis, which is mainly due to too strong noise or total response strength. These findings provide new insights into the stability and dynamics of "hubs," a motif in interaction networks that is essential for understanding and managing real-world complex systems.

I. INTRODUCTION

In many complex systems, the concept of a hub—an entity that interacts with and influences numerous other entities—is central to understanding the collective and characteristic properties of the whole systems. This hub-based dynamic is prevalent across a wide range of fields, including power networks [1], logistics or transportation [2, 3], markets [4], and ecology [5]. In power networks, the dynamics of a central power station (the hub) significantly impact the stability and efficiency of the entire grid, as it regulates the distribution of electricity to numerous nodes. Similarly, in logistics and transportation, major hubs such as distribution centers or transportation hubs coordinate the flow of goods and passengers, affecting the efficiency and reliability of the entire network. The stock market is another prime example, where the stock price of a key company can act as a hub, influencing the actions of numerous investors and traders. These interactions, characterized by buying and selling activities, shape the dynamics of the stock market and determine its behavior. In the field of ecology, certain global environmental factor is like a hub mediating the interactions of all species (like pH for bacteria).

Given the central role hubs play in these diverse systems, understanding their dynamics is of paramount importance. The dynamics of the hub are particularly critical, as they often determine the overall behavior and stability of the system. By focusing on the hub's dynamics, we can gain insights into the mechanisms driving system-wide changes and develop strategies to manage or optimize these complex systems.

In this study, starting from the idea of modeling an interaction network motif—many individuals interacting with one hub—we propose a simple stochastic delay differential equation (SDDE) framework that focuses solely on the dynamics of the hub. This approach is motivated by the common occurrence of such motifs in fields like ecology, transportation, and economy. The delayed dynamics in our model captures the reciprocal influence where the hub affects the connected entities, which in turn affect the hub back. The inclusion of stochastic noise accounts for various factors, including the consequences of weak interactions directly between the entities. Through both numerical simulations and theoretical analysis, we investigate the emergent dynamics, revealing a range of behaviors such as stable states, limit cycles, and chaos.

II. SETUP

We consider the dynamics of the hub being governed by a SDDE

$$\dot{x} = h - \sum_i b_i x(t-\tau_i) - ax^3 + \eta(t). \tag{1}$$

The constant h reflects the averaged effects by all the entities. The quantity $x(t-\tau_i)$ is related to the value at t of the ith entity connected to the hub, the delay time τ_i reflects how fast the ith entity response to the hub x. The delayed response is the easiest way if we only want to write down dynamics of the hub while want to include the effects of the entities interacting with the hub. The quantity b_i encodes how strong entity i affect back on the hub which will be referred to as the response strength. The term ax^3 is needed to ensures that x is bounded, while higher order terms are neglected as we focus on

* liuyz@mit.edu

small $|x|$ sufficing to describe dynamical transitions. The while noise η is assumed to have $\langle \eta(t)\eta(t')\rangle = \lambda\delta(t-t')$. The noise can include many things including some effects due to direct but weak interactions among the entities.

One specific scenario is to consider x as the pH level of a solution, with the entities being bacteria abundances. The pH level x affects bacterial growth, and the bacterial populations in turn affect the pH level. The regulation of pH is delayed, as changes in bacterial growth rates take time to impact the overall population. This delayed regulation is a negative feedback mechanism: when the pH becomes too low or too high, it reduces bacterial populations, thereby decreasing the production of acidic or alkaline metabolites that would otherwise further alter the pH. The constant h reflects the averaged effect of all bacteria on the pH. The term $x(t-\tau_i)$ represents the delayed effect of the ith bacterial population on the pH level, with τ_i indicating the response time. The response strength b_i encodes how strongly the ith bacterial population influences the pH. The non-linear term ax^3 ensures that the pH remains within a biologically viable range, while higher-order terms are neglected as we focus on small values of $|x|$. The white noise $\eta(t)$ accounts for various sources of randomness, including weak interactions among different bacterial populations and environmental fluctuations.

Another example is the stock market, where the stock price of a company can be considered as the hub x, and the agents (investors, traders, and institutions) are interacting with this hub through buying and selling actions. The stock price x is influenced by the cumulative effect of these agents' actions, represented by the constant h, which reflects the averaged impact of all market participants. The term $x(t-\tau_i)$ captures the delayed response of the ith agent to the stock price, where the delay time τ_i represents how quickly the agent reacts to changes in the stock price. The response strength b_i encodes the influence of the i-h agent's actions on the stock price. The non-linear term ax^3 ensures that the stock price remains bounded, reflecting real-world constraints and market regulations. The stochastic term $\eta(t)$ represents various sources of market noise, including economic news, investor sentiment, and other external factors. This model captures the dynamic interplay between stock prices and agent behaviors, highlighting the delayed and stochastic nature of market interactions.

III. RESULTS

We first explored the possible dynamics the model can display. We chose ten lag times τ_i from a truncated Gaussian distribution given the same response strength b_i and ran simulations varying the common response strength b_i and noise strength λ (see Appendix. D). We observed that there can be three different behaviors, one is being (robustly) stable (at a fixed point), another one is being in (robust) limit cycles, and the last one is chaos

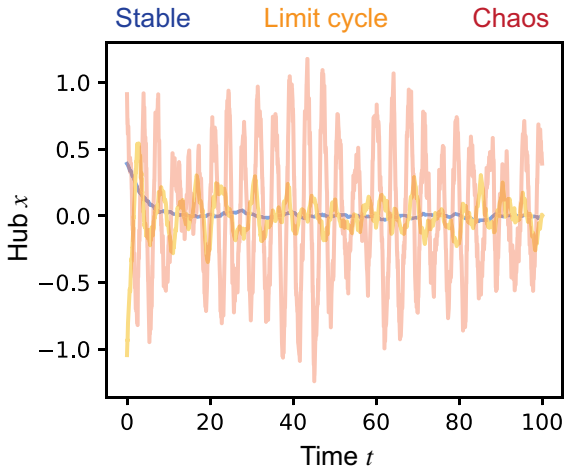

FIG. 1. Proposed model for the hub of interaction can display all kinds of dynamics. If the dominant peak frequency is zero and Lyapunov exponent is negative, we classify the dynamics as (robustly) stable, which is demonstrated as the blue curve. If the peak frequency is non-zero and Lyapunov exponent is negative, the dynamics is classified as a (robust) limit cycle (yellow curve is an example). And if the Lyapunov exponent is positive, dynamics is chaotic with the red curve as an example.

(Fig. 1). The word "robust" here means the behavior is robust to noise added. To be more specific, we used time series analysis to estimate the Lyapunov exponent from data (see Appendix. D) [6]. If the Lyapunov exponent is greater than zero, we classify the time series as chaotic which may due to the deterministic part of our dynamics or the noise. If we obtained a negative Lyapunov exponent, it means we can well predict the time series from data and therefore the dynamics is robust to noise. We further analyzed the peak frequency of the Fourier transformed time series, with zero peak frequency corresponding to being stable at fixed points and non-zero peak frequency referring to limit cycles. In fact, there might be more detailed classification as limit cycle or chaos can be due to noise (i.e., cannot show up without noise) or due to the intrinsic part. We conclude that the simple dynamics can display full range of dynamics relevant to observed time series, including being stable (short for being robustly stable at the fixed point), limit cycles (short for robust limit cycles), and chaos.

To build a basic picture for the emergence of different kinds of dynamics, we next make several assumptions for analyticity. First of all, h is set to be 0 in this project. We also assume the response strengths b_i are all positive, such that the responses are all negative autoregulation. Negative response strengths in general may lead to more diverse dynamical behaviors (see IV. Discussion) [7]. I thought it was impossible to analyze the negative response strengths within the scheme I am going to introduce but actually possible (something to work on after the deadline). We can introduce a distribution

for delay time τ based on the positive response strengths then as

$$\rho_b(\tau) \equiv \frac{1}{\zeta}\sum_i b_i \delta(\tau - \tau_i), \tag{2}$$

where $\zeta = \sum_i b_i$ is the total response strength. Since we are interested in cases where there are many entities connected to the hub, we can use a continuous distribution to approximate $\rho_b(\tau)$ in analysis. Furthermore, we assume the continuous distribution to be a truncated Gaussian (the distribution is truncated at zero since $\tau > 0$, otherwise it means future can affect the present). Formally, we say ρ_b is the probability density function for

$$\tau = \max\{\tau^+, 0\},\ \tau^+ \sim \mathcal{N}(\mu, \sigma^2). \tag{3}$$

We believe that choosing other distributions will not change the qualitative picture. We use the truncated Gaussian distribution in numerical studies while directly use the Gaussian distribution ($\mathcal{N}(\mu, \sigma^2)$) in theoretical calculation for simplicity. Based on the assumptions, our model can be rewritten as

$$\dot{x} = -\zeta \int \mathrm{d}\tau \rho_b(\tau) x(t-\tau) - ax^3 + \eta(t). \tag{4}$$

We therefore expect the dynamical behaviors will be determined by total response strength ζ, mean delay time μ, standard deviation of delay time σ, non-linear response strength a, and noise strength λ.

With the specified model, we then did a detailed exploration into different dynamics and transitions. We fixed $\mu = 1$, $\sigma = 0.5$, $a = 1$, but varied total response strength ζ (50 values in $[0, 4]$) and noise strength λ (50 values in $[0, 0.3]$). For each given pair of ζ and λ values, we randomly sampled 10 initial conditions from which we ran for time 100 (this time is long enough for most frequencies in fluctuations observed, see more details in Appendix. D). The Fourier transformed time series, denoted as $x(\omega)$ where ω is the (angular) frequency, were calculated to estimate $\langle |x(\omega)|^2 \rangle$. We defined the peak frequency as

$$\omega_m = \arg\max_{\omega} \langle |x(\omega)|^2 \rangle, \tag{5}$$

and observed ω_m mainly depends on the total response strength ζ (Fig. 2a). From the time series $x(t)$, we can estimate the Lyapunov exponent. The averaged Lyapunov exponents over 10 trajectories from different initial condition for the same ζ and λ are found to have a complicated dependence on ζ and λ (Fig. 2b). Since we have zero and non-zero peak frequencies as well as negative and positive Lyapunov exponents on the diagrams, we are able to identify the regimes for stability, limit cycles, and chaos.

We next started to study the simple pattern of peak frequencies or the most likely frequencies observed. The distribution of a path $x(t)$, denoted by $P[x(t)]$, can be derived, which further can give the distribution of Fourier

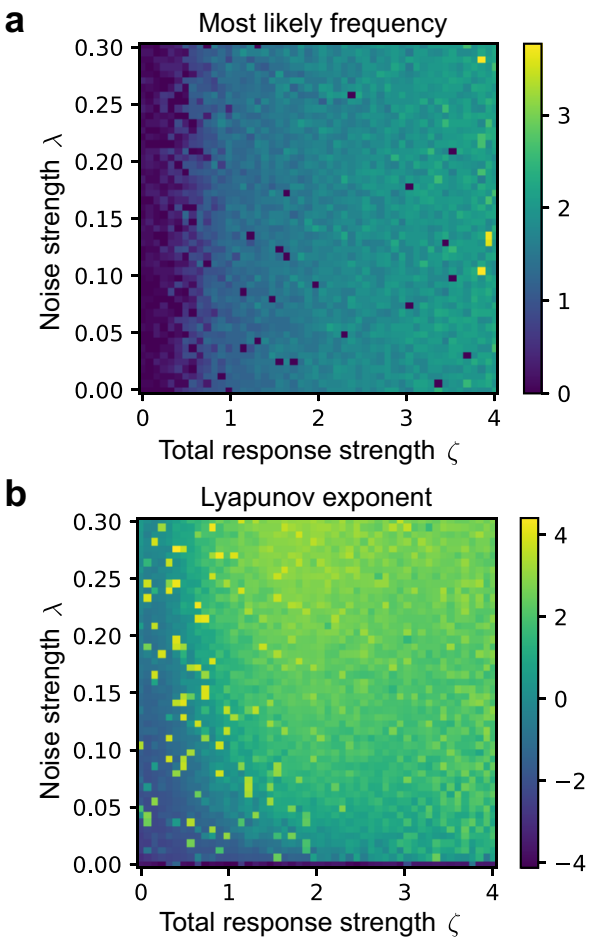

FIG. 2. Dynamical behaviors depend on response strength and noise strength. (a) Heatmap showing the most likely frequency as a function of total response strength ζ and noise strength λ. Higher frequencies are observed with increasing total response strength. (b) Heatmap illustrating the Lyapunov exponent as a function of total response strength ζ and noise strength λ. Positive Lyapunov exponents, indicating chaos, become more prevalent with increasing noise strength and response strength. The color bars indicate the values of the most likely frequency and Lyapunov exponent, respectively.

modes, $P[x(\omega)]$ (see Appendix. B). If we only look at the Gaussian part of the distribution $P[x(\omega)]$, which corresponds to only keeping linear terms in the original dynamics, we obtained a simple Gaussian distribution $P_0[x(\omega)]$ giving

$$\langle |x(\omega)|^2 \rangle_0 = \frac{\lambda}{\Psi - 3\lambda a}, \tag{6}$$

where $\langle \cdot \rangle_0$ denote the mean with respect to $P_0[x(\omega)]$ and

$$\Psi = \omega^2 + \zeta^2 e^{-\omega^2\sigma^2} - 2\zeta\omega e^{-\frac{\omega^2\sigma^2}{2}} \sin(\omega\mu). \tag{7}$$

Note that Ψ has the above explicit form as we used Gaussian ρ_b rather than truncated Gaussian distribution in

theoretical calculation. If the analysis based on Gaussian part $P_0[x(\omega)]$ is valid, the most likely frequency can be estimated as

$$\omega_m \approx \arg\min_{\omega} \Psi, \tag{8}$$

which is 0.47 given values we set $\mu = 1$ and $\sigma = 0.5$. We numerically calculated the value, which in theory only depends on ζ, μ, and σ based on the formula of Ψ, and compared the theory with simulation data (see Fig. 3a, where the dark line is theoretical prediction and dots with same color come from the same λ values). The results suggest that peak frequencies observed agrees well with the theory but have weak dependence on λ. From theory and data, there is a continuous phase transition with increasing ζ, corresponding to the emergence of non-zero ω_m (i.e., non-zero minima of Ψ) or the transition to limit cycles from being stable. We can identify the critical value ζ_l for this transition via $\frac{\partial^2 \Psi}{\partial \omega^2}|_{\omega=0} = 0$ (see Appendix. C):

$$\zeta_l = \frac{-\mu + \sqrt{\mu^2 + \sigma^2}}{\sigma^2}. \tag{9}$$

As will be shown, the data obtained include cases where the Gaussian part $P_0[x(\omega)]$ is unstable or divergent, or the linear terms of dynamics lose stability such that the non-linear part is required to make the dynamics bounded. However, the peak frequency obtained from the Gaussian model seems to still be valid. When the Gaussian part becomes unstable, its peak frequency is close to that of the fastest diverging mode which will dominate the dynamics even in the non-linear regime. So, the dominant frequency observed will still be similar to that from the Gaussian part analysis. We therefore conclude that with the Gaussian part of path probability (or linear terms of the dynamics), we can well explain and predict the dominant frequencies in all dynamics.

We next sought to study in detail the validity of the Gaussian model $P_0[x(\omega)]$ and its connection to dynamical behaviors. The critical case when the Gaussian model loses stability intuitively corresponds to $\langle |x(\omega)|^2 \rangle_0 = \infty$ for some ω. We therefore can find the critical noise strength for the Gaussian model to lose stability as

$$\lambda_c(\zeta) = \frac{1}{3a} \min_{\omega} \Psi. \tag{10}$$

We plotted this λ_c as a function of ζ (red curve) along with the dynamical phase diagram (Fig. 3b), where stability (blue), limit cycles (yellow), and chaos (orange) are classified based on peak frequency (Fig. 2a) and Lyapunov exponent (Fig. 2b) as explained. The results suggest that λ_c can distinguish limit cycles from chaos in a range of ζ approximately from 0.8 to 2.1, and seems to have no connection to dynamical behaviors observed for other ζ values. The upper critical ζ value where λ_c begin not to distinguish limit cycles and chaos seems to be the point where $\lambda_c = 0$. To understand this, we can think about complex value ω where the imaginary part means divergence or convergence rate. The function Ψ can always reach zero for certain complex ω. When ζ is small, the complex ω values making Ψ zero has positive real imaginary part, suggesting stability or convergence only due to the linear terms in dynamics. At this regime, if we increase λ, we will have instability when there are ω with negative imaginary part making $\Psi - 3\lambda a$ zero, leading to the critical point identified by $\Psi - 3\lambda a = 0$ for some real ω and giving $\lambda_c(\zeta)$. However, when ζ is large, the complex ω making Ψ zero will begin to have negative imaginary part, suggesting intrinsic instability even without any noise. In this case, $\Psi - 3\lambda a = 0$ for some real ω no longer corresponds to instability. The transition to intrinsic instability (of the Gaussian part) happens when we can have $\Psi = 0$ for some real ω, i.e., when $\lambda_c = 0$. The critical ζ_c (in our range of interest) is given by (see Appendix. C)

$$\zeta_c = \frac{\pi}{2\mu} e^{\frac{\pi^2 \sigma^2}{8\mu^2}}, \tag{11}$$

which is 2.1 for $\mu = 1$ and $\sigma = 0.5$ we set. We therefore plotted $\lambda_c(\zeta)$ beyond this ζ_c as a dashed curve since it no longer identifies the instability. Interestingly, we found when there is no noise at all, the dynamics go to limit cycles when the linear terms lose stability (beyond ζ_c). For the part ζ approximately smaller than 0.8, there seems to be no consequence after the Gaussian part loses stability, i.e., the dynamical phases are continuous when we increase λ to pass λ_c (red curve). We may interpret this phenomena as ζ is still weak and even the noise can make Gaussian part unstable, the non-linear term in dynamics can well regulate the system to staying in the same dynamical phase. We therefore conclude that the loss of stability of the Gaussian model is partly related to transition to chaos.

Gathering all the information, we can summarize our dynamical phase diagram observed. In the range of λ and ζ we were studying, before ζ_c, the Gaussian model instability is driven by noise, and therefore the instability boundary is given by $\lambda_c(\zeta)$ (red curve in Fig. 3b). When $\zeta < \zeta_c$ while greater than certain value, the loss of Gaussian model stability corresponds to transition to chaos. For other smaller ζ, transition to chaos is determined by non-linear terms in the dynamics which have not been analyzed. After ζ_c, the Gaussian part is intrinsically unstable, where when $\lambda = 0$, the dynamics is in limit cycles sustained by non-linear regulation, and when $\lambda > 0$, the dynamics is chaotic. We expect certain renormalization procedure can identify the transition to chaos dominant by non-linear effects. The transition from stability to limit cycles is well identified by ζ_l estimated from the Gaussian part (dark vertical line in Fig. 3b) which works robustly even after the Gaussian part loses stability. The dynamical phase diagram is therefore partly explained and understood through the Gaussian model analysis.

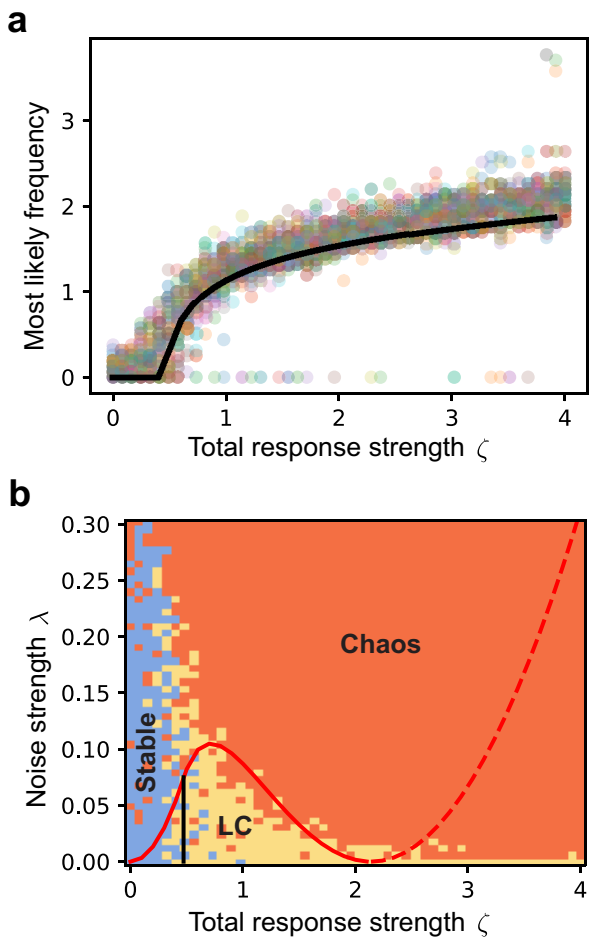

FIG. 3. Gaussian model analysis robustly explains peak frequency observed and dynamical phase diagram. (a) Scatter plot showing the most likely frequency as a function of total response strength ζ, with the black line representing the Gaussian model's prediction. The model accurately captures the increase in peak frequency with growing response strength. (b) Phase diagram depicting different dynamical regimes as functions of total response strength ζ and noise strength λ. The regions labeled "Stable," "LC" (Limit Cycles), and "Chaos" indicate the respective dynamical behaviors. The dark solid line encodes ζ_l where peak frequency becomes non-zero, such that it identifies transition to limit cycles. The red curve is the λ_c as a function of ζ identifying when the Gaussian part loses stability. Beyond $\zeta_c \approx 2.1$, the curve is dashed as the Gaussian part is intrinsically unstable without noise beyond ζ_c and λ_c does not correspond to instability of Gaussian part anymore. The instability of the Gaussian model partly corresponds to transition to chaos (ζ approximately between 0.8 and ζ_c) with other chaotic transition related to higher non-linear terms.

IV. DISCUSSION

Starting from the idea to model an interaction network motif, i.e., many individuals interacting with one hub, which are common in fields like ecology, transportation, and economy, we proposed a simple SDDE framework concerning only the dynamics of the hub. The delayed dynamics is to model the fact hub affects the connected entities which affect the hub back. And the stochastic noise includes all other factors including consequences due to some weak interactions directly between the entities. Through numerical and theoretical study, we observed and partly explained the emergent dynamics including stable states, limit cycles, and chaos.

The limitation of our model is that we have too many assumptions at first place. For example, we now only studied the case where $h = 0$ (see Eq. (1)), distribution ρ_b is truncated Gaussian, and all the delayed responses are negative auto-regulation. We believe the last one assumption can be easily removed and can lead to more interesting and qualitatively different behaviors. We may assume two continuous distributions later: one for negative feedback, and one for positive feedback. There are potentially more complicated phase diagram with respect to total negative response strength and total positive response strength.

Our numerical analysis of Lyapunov exponent is quite phenomenological. We fed the algorithm time series from a stochastic process while the algorithm was designed to deal with deterministic dynamics. The intuition is that if this Lyapunov exponent calculated is small, it means the noise does not alter the original dynamics much and we should have (robust) stable states or limit cycles. However, it remains a question how to define chaos or Lyapunov exponent for a stochastic dynamics properly. Actually, there are two specific questions: one is how to define chaos phase or what is the proper order parameter in our theoretical analysis; and another is if there is a connection between this theoretically defined chaos phase (may be related to fixed point of renormalization, $\lambda = \infty$ and $\zeta = 0$) and the one identified though numerically calculated Lyapunov exponent.

Going beyond the analysis of Gaussian part of the path probability or the linear terms of the dynamics, we may be able to define chaos and explain transition to chaos observed in simulation. The first thought was to apply renormalization analysis. While the nonlinear terms in the path probability are quite complex. I am not certain if perturbative renormalization procedure can work as the factors before the non-linear terms actually are of the same order as those of the quadratic terms or the Gaussian part (see Appendix. B).

In general, the SDDE framework is simple in terms of the form but can show quite diverse behaviors. We anticipate the model to be useful in understanding some real data and providing a basis of thinking.

ACKNOWLEDGEMENTS

It is a pleasure to thank Jiliang Hu, Jinyeop Song, and Jeff Gore for discussions on pH, Sunghan Ro and Mehran Kardar for suggestions on model construction, Josh Liu for help on numerical techniques.

[1] D. Bian and Y. Chen, Dynamic modeling and analysis of smart grid technologies and the power market, Energy Economics **57**, 1 (2016).
[2] D. Thorpe and R. Mitra, *System Dynamics Modeling of Logistics Hub Capacity: The Dubai Logistics Hub* (Springer, 2011).
[3] e. a. Cao, K., Towards the sustainable development of logistics system model: A system dynamics approach, PLOS ONE **16**, e0249043 (2021).
[4] J. D. Farmer and J. Geanakoplos, The virtues and vices of equilibrium and the future of financial economics, Complexity **14**, 11 (2009).
[5] C. Ratzke, J. Barrere, and J. Gore, Strength of species interactions determines biodiversity and stability in microbial communities, Nature Ecology & Evolution **4**, 376 (2020).
[6] M. T. Rosenstein, J. J. Collins, and C. J. De Luca, A practical method for calculating largest lyapunov exponents from small data sets, Physica D: Nonlinear Phenomena **65**, 117 (1993).
[7] D. S. Glass, X. Jin, and I. H. Riedel-Kruse, Nonlinear delay differential equations and their application to modeling biological network motifs, Nature Communications **12**, 1788 (2021).
[8] K. Sekimoto, *Stochastic Energetics*, Lecture Notes in Physics, Vol. 799 (Springer, Berlin, Heidelberg, 2010).
[9] A. Reuther, J. Kepner, C. Byun, S. Samsi, W. Arcand, D. Bestor, B. Bergeron, V. Gadepally, M. Houle, M. Hubbell, M. Jones, A. Klein, L. Milechin, J. Mullen, A. Prout, A. Rosa, C. Yee, and P. Michaleas, Interactive Supercomputing on 40,000 Cores for Machine Learning and Data Analysis, in *2018 IEEE High Performance Extreme Computing Conference (HPEC)* (2018) pp. 1–6.

Appendix A: Preliminaries

We summarize conventions used in the derivation. For Fourier transform, we use the following convention

$$\begin{cases} x(\omega) = \int \mathrm{d}t e^{-\mathrm{i}\omega t} x(t), \\ x(t) = \int \dfrac{\mathrm{d}\omega}{2\pi} e^{\mathrm{i}\omega t} x(\omega). \end{cases} \tag{A1}$$

In principle, we need to use a new symbol (like $\tilde{x}$) to indicate the Fourier modes. But for simplicity, we use the same symbol while explicitly write the argument t or ω to indicate it is in time domain (original time series) or frequency domain (Fourier modes). We also used the not italic symbol i for imaginary unit. We will use the symbol $\mathcal{D}$ for functional integral or differentiation.

Appendix B: Probability of a path

We consider the probability of a path $x(t)$ for special case $h = 0$. To start, the noise have probability

$$P[\eta(t)] \propto \exp\left(-\frac{1}{2\lambda}\int \eta^2(t)\mathrm{d}t\right). \tag{B1}$$

Substituting η by variables related to x (rearrange Eq. (1)) and taking care of the change of variable, the same probability is rewritten in terms of x:

$$P[x(t)] \propto \exp\left(-\frac{1}{2\lambda}\int \left(\dot{x} + \sum_i b_i x(t-\tau_i) + ax^3\right)^2 \mathrm{d}t\right) \det J, \tag{B2}$$

where the Jacobian $J = \mathcal{D}\eta/\mathcal{D}x$.

We next evaluate the Jacobian through a heuristic way. We discretize our dynamics (Eq. (1)) in time with time step Δt as

$$\Delta x_n = -\frac{1}{2}(\sum_i b_i x_{n-n_i} + ax_n^3)\Delta t - \frac{1}{2}(\sum_i b_i x_{n+1-n_i} + ax_{n+1}^3)\Delta t + \Delta\eta_n \tag{B3}$$

$$= -(\sum_i b_i x_{n-n_i} + ax_n^3)\Delta t - \frac{1}{2}(\sum_i b_i \Delta x_{n-n_i} + 3ax_n^2\Delta x_n)\Delta t + \Delta\eta_n \tag{B4}$$

where $\Delta x_n = x_{n+1} - x_n$. Since $\langle \Delta\eta_n \Delta\eta_m \rangle = \delta_{n,m}\lambda\Delta t$, we can regard $\Delta\eta_n \sim \sqrt{\Delta t}$. This discretization rule follows the Stratonovich stochastic calculus and assures the correct limit when $\Delta t \to 0$ [8]. If we use Itô calculus, the first step in discretization needs to use Itô's lemma, which will give the same finial result. The Jacobian elements are given by

$$J_{nn} = \frac{\partial \Delta\eta_n}{\partial \Delta x_n} = 1 + \frac{3}{2} a x_n^2 \Delta t. \tag{B5}$$

The off-diagonal elements are all of order Δt which will be negligible when $\Delta t \to 0$. We therefore have

$$\det J \approx \prod_n (1 + \frac{3}{2} a x_n^2 \Delta t) \approx \exp\Big(\sum_n \frac{3}{2} a x_n^2 \Delta t \Big) \approx \exp\Big(\int \frac{3}{2} a x^2(t) \mathrm{d}t \Big), \tag{B6}$$

and finally

$$P[x(t)] \propto \exp\left(-\frac{1}{2\lambda} \int \left[\Big(\dot{x} + \sum_i b_i x(t-\tau_i) + a x^3 \Big)^2 - 3\lambda a x^2 \right] \mathrm{d}t \right). \tag{B7}$$

We then transform to frequency domain to study the distribution of Fourier modes $x(\omega)$, from which the phase transition can be clear. We essentially need to study the Fourier transform of the following quantity

$$H[x(t)] \equiv \Big(\dot{x} + \sum_i b_i x(t-\tau_i) + a x^3 \Big)^2 - 3\lambda a x^2 \tag{B8}$$

$$= \dot{x}^2 + a^2 x^6 + \sum_{i,j} b_i b_j x(t-\tau_i) x(t-\tau_j) + 2a\dot{x}x^3 + 2\dot{x} \sum_i b_i x(t-\tau_i) + 2a x^3 \sum_i b_i x(t-\tau_i) - 3\lambda a x^2. \tag{B9}$$

We study the terms one by one. The first term in the last row of the above equation, $\dot{x}^2$, has a contribution as:

$$\int \dot{x}^2(t) \mathrm{d}t = \int \frac{\mathrm{d}\omega}{2\pi} \omega^2 |x(\omega)|^2. \tag{B10}$$

The second term essentially depends on

$$\int x^6(t) \mathrm{d}t = \int \frac{\mathrm{d}\omega_1 \mathrm{d}\omega_2 \mathrm{d}\omega_3 \mathrm{d}\omega_4 \mathrm{d}\omega_5}{(2\pi)^5} x(\omega_1) x(\omega_2) x(\omega_3) x(\omega_4) x(\omega_5) x(-\omega_1 - \omega_2 - \omega_3 - \omega_4 - \omega_5). \tag{B11}$$

The third term and the last term (can be thought as setting $\tau_i = \tau_j = 0$ for the third term) require us to evaluate

$$\int x(t-\tau_i) x(t-\tau_j) \mathrm{d}t = \int \frac{\mathrm{d}\omega}{2\pi} e^{-\mathrm{i}\omega\tau_i + \mathrm{i}\omega\tau_j} |x(\omega)|^2 = \int \frac{\mathrm{d}\omega}{2\pi} \cos(\omega(\tau_j - \tau_j)) |x(\omega)|^2. \tag{B12}$$

The fourth term has the transformation

$$\int \dot{x}(t) x^3(t) \mathrm{d}t = \int \frac{\mathrm{d}\omega_1 \mathrm{d}\omega_2}{(2\pi)^3} \mathrm{i}\omega_1 x(\omega_1) x(\omega_2) x(\omega_3) x(-\omega_1 - \omega_2 - \omega_3). \tag{B13}$$

The fifth term depends on the transformation

$$\int \dot{x}(t) x(t-\tau_i) \mathrm{d}t = \int \frac{\mathrm{d}\omega}{2\pi} \mathrm{i}\omega e^{\mathrm{i}\omega\tau_i} |x(\omega)|^2 = \int \frac{\mathrm{d}\omega}{2\pi} (-\omega) \sin(\omega\tau_i) |x(\omega)|^2. \tag{B14}$$

The sixth term needs us to evaluate transformation like

$$\int x^3(t) x(t-\tau_i) \mathrm{d}t = \int \frac{\mathrm{d}\omega_1 \mathrm{d}\omega_2}{(2\pi)^3} e^{\mathrm{i}(\omega_1 + \omega_2 + \omega_3)\tau_i} x(\omega_1) x(\omega_2) x(\omega_3) x(-\omega_1 - \omega_2 - \omega_3). \tag{B15}$$

The terms with degree higher than 2 are regarded as interactions between modes, which may be studied through a perturbative way. We then first study the quadratic terms, i.e., the Gaussian model.

Appendix C: Gaussian part analysis

We extract all the quadratic terms first such that we obtain a Gaussian distribution for Fourier modes neglecting their interactions:

$$P_0[x(\omega)] \propto \exp\left(-\frac{1}{2\lambda}\int \frac{\mathrm{d}\omega}{2\pi}\Big[\omega^2 + \sum_{i,j} b_i b_j \cos(\omega(\tau_j-\tau_j)) - 2\sum_i b_i\omega\sin(\omega\tau_i) - 3\lambda a\Big]|x(\omega)|^2\right) \tag{C1}$$

We can read out the corresponding correlation function

$$\langle x(\omega)x(\omega')\rangle_0 = \frac{2\pi\delta(\omega+\omega')\lambda}{\omega^2 + \sum_{i,j} b_i b_j \cos(\omega(\tau_j-\tau_j)) - 2\sum_i b_i\omega\sin(\omega\tau_i) - 3\lambda a}. \tag{C2}$$

It suffices to focus on

$$\langle|x(\omega)|^2\rangle_0 \equiv \frac{\lambda}{\omega^2 + \sum_{i,j} b_i b_j \cos(\omega(\tau_j-\tau_j)) - 2\sum_i b_i\omega\sin(\omega\tau_i) - 3\lambda a}, \tag{C3}$$

or simply

$$R_0(\omega) \equiv \omega^2 + \sum_{i,j} b_i b_j \cos(\omega(\tau_j-\tau_j)) - 2\sum_i b_i\omega\sin(\omega\tau_i) - 3\lambda a \tag{C4}$$

$$= \omega^2 + \zeta^2\overline{\cos(\omega(\tau-\tau'))} - 2\zeta\omega\overline{\sin(\omega\tau)} - 3\lambda a. \tag{C5}$$

Here, we use the over bar $\bar{\cdot}$ to denote mean values associated to the density $\rho_b(\tau)$:

$$\rho_b(\tau) \equiv \sum_i b_i\delta(\tau-\tau_i)/\zeta,\ \zeta = \sum_i b_i. \tag{C6}$$

The density ρ_b is interpreted as distribution of response strength over response time, and ζ is the total response strength. When there are a large number of entities interacting with one hub, we can approximate ρ_b via a continuous distribution in analysis.

We next substitute $\rho_b(\tau)$ as the probability density function for Gaussian distribution $\mathcal{N}(\mu,\sigma)$ and analyze the behaviors. We first can rewrite R_0 based on the Fourier transform of the function $\rho_b(\tau)$, which is denoted as $\rho_b(\omega)$:

$$R_0(\omega) = \omega^2 + \zeta^2|\rho_b(\omega)|^2 + 2\zeta\omega\mathrm{Im}(\rho_b(\omega)) - 3\lambda a. \tag{C7}$$

Note for Gaussian distribution

$$\rho_b(\tau) = \frac{1}{\sqrt{2\pi}\sigma}e^{-\frac{\tau^2}{2\sigma^2}}, \tag{C8}$$

the Fourier modes is given by

$$\rho_b(\omega) = e^{-\frac{\omega^2\sigma^2}{2}}e^{-\mathrm{i}\omega\mu}, \tag{C9}$$

we can obtain

$$R_0(\omega) = \omega^2 + \zeta^2 e^{-\omega^2\sigma^2} - 2\zeta\omega e^{-\frac{\omega^2\sigma^2}{2}}\sin(\omega\mu) - 3\lambda a. \tag{C10}$$

By defining

$$\Psi \equiv \omega^2 + \zeta^2 e^{-\omega^2\sigma^2} - 2\zeta\omega e^{-\frac{\omega^2\sigma^2}{2}}\sin(\omega\mu), \tag{C11}$$

we proceed to identify the transition to non-zero peak frequency as explained in the main text. The critical condition $\frac{\partial^2\Psi}{\partial\omega^2}|_{\omega=0} = 0$ can be expanded as

$$2 - 2\zeta^2\sigma^2 - 4\zeta\mu = 0, \tag{C12}$$

giving the critical ζ_l as its positive root

$$\zeta_l = \frac{-\mu + \sqrt{\mu^2 + \sigma^2}}{\sigma^2}. \tag{C13}$$

We next analyze the intrinsic instability of the Gaussian model, which means the linear part of the dynamical model will lead to divergence and this instability will happen without any noise. We can have such instability when $\Psi(\omega) = 0$ has a complex solution whose imaginary part is negative. The critical transition to this intrinsic instability then correspond to the case where $\Psi(\omega) = 0$ has a real solution. We found Ψ can be written as

$$\Psi = \left| \mathrm{i}\omega - \zeta e^{-\frac{\omega^2\sigma^2}{2}} e^{\mathrm{i}\omega\tau} \right|^2, \tag{C14}$$

which leads to

$$\omega = \zeta e^{-\frac{\omega^2\sigma^2}{2}} \sin(\omega\mu),\ \zeta e^{-\frac{\omega^2\sigma^2}{2}} \cos(\omega\mu) = 0, \tag{C15}$$

if we want $\Psi = 0$ for some real ω. We then can solve from above equations for possible non-zero ζ at these critical transitions

$$\zeta_n = \frac{\pi}{\mu}\left(\frac{1}{2} + 2n\right) e^{(\frac{1}{2}+2n)^2 \frac{\pi^2\sigma^2}{2\mu^2}},\ n = 0, 1, 2, ... \tag{C16}$$

The full picture is that when ζ is below ζ_0, the system is intrinsically stable, and the Gaussian part is intrinsically unstable when $\zeta_0 < \zeta < \zeta_1$, but it goes back to be stable when $\zeta_1 < \zeta < \zeta_2$... In the main text, our ζ_c is actually ζ_0 defined above and ζ_1 is far beyond the range we numerically tested so we did not mention.

Appendix D: Numerical methods

We conducted scale numerical simulations with Julia 1.8.5 on MIT Supercloud [9], ran small scale tests and analyze data with Python 3.10.9 and MATLAB R2023a on a laptop. All codes are available online. In practice, we sampled 10 delay time τ_i from the given truncated Gaussian distribution $\rho_b(\tau)$. We set $b_i = \zeta/10$ such that total response strength is ζ. The initial condition $x(0)$ is randomly sampled from $\mathcal{N}(0, 1)$. We simulate each case for $t = 100$, and output x at 2^{13} evenly distributed time points in $[0, 100]$ for analysis.

To analyze the time series, we used standard fast Fourier transform in Python to find the peak frequency. We estimated the Lyapunov exponent from time series with the function `lyapunovExponent` in MATLAB. The idea is to use delayed embedding to reconstruct the phase space of a dynamical system from a time series and then estimate how fast neighboring points in the phase space will diverge or converge [6]. This method involves creating a set of vectors from the time series by using delayed copies of the data. Formally, for a time series $x(t)$, we construct vectors of the form $[x(t), x(t-\tau), x(t-2\tau), \ldots, x(t-(m-1)\tau)]$, where τ is the time delay and m is the embedding dimension. This reconstructed phase space preserves the dynamical properties of the original system, allowing us to analyze its behavior and estimate key quantities such as the Lyapunov exponent. The Lyapunov exponent measures the average rate of separation of infinitesimally close trajectories, providing insight into the system's sensitivity to initial conditions and its chaotic nature. If this estimated Lyapunov exponent is small, it effectively suggests that we can well predict the dynamics without any model but just with data collected.